Hindawi
Wireless Communications and Mobile Computing
Volume 2022, Article ID 2673024, 13 pages
https://doi.org/10.1155/2022/2673024

Research Article

Performance of Spectrum Sharing in Hybrid Satellite Terrestrial Network with Opportunistic Relay Selection

Guanchang Xue,[1] **Mingchuan Yang**,[1] **Qing Guo**,[1] **and Shuai Yuan**[2]

[1]*Communication Research Center, Harbin Institute of Technology, Harbin 150001, China*
[2]*Qian Xuesen Laboratory of Space Technology, China Academy of Space Technology, Beijing 100000, China*

Correspondence should be addressed to Mingchuan Yang; mcyang@hit.edu.cn

Received 17 May 2022; Accepted 6 September 2022; Published 14 October 2022

Academic Editor: Haitao Xu

Copyright © 2022 Guanchang Xue et al. This is an open access article distributed under the Creative Commons Attribution License, which permits unrestricted use, distribution, and reproduction in any medium, provided the original work is properly cited.

In this paper, we consider the uplink of a hybrid satellite-terrestrial spectrum sharing system, in which satellite terminal communicates with satellite through terrestrial relay-assisted transmission. To accommodate expanding networks within limited spectrum, spectrum sharing is considered a promising candidate. For the system in which satellite terminals and terrestrial terminals share spectrum, we propose opportunistic relay selected spectrum sharing method based on decoding and forwarding protocol. Selecting the optimal relay station is aimed at minimizing the outage probability of the satellite terminal and maximizing the throughput of the system. Due to spectrum sharing policy and imperfections in the RF front end, we also consider the effects of cochannel interference (CCI) and hardware impairments (HIs). The satellite link is modeled as Shadowed-Rician fading, and the terrestrial link uses Nakagami-m fading. In addition, we deduce the closed-form analytical expressions of the satellite terminal outage probability, deduce the asymptotic expressions under the condition of high signal-to-noise ratio, and analyze their achievable diversity orders. Numerical and simulation results validate the performance gain of opportunistic relay selection compared to partial relay selection. Monte Carlo simulations confirm the correctness of the theoretical analysis and illustrate the effects of CCI and HIs on the system.

1. Introduction

Integrating satellite networks and terrestrial networks to build a three-dimensional network with seamless global coverage has become an important direction for the development of sixth generation (6G) network technology and has become a research hotspot in the current academic and industrial circles [1]. Today, both satellite and terrestrial networks are rapidly expanding to meet growing demands for higher throughput, lower latency, and wider coverage. However, the scarcity of spectrum presents an obstacle to sustainable development. To accommodate expanding networks within limited spectrum, spectrum sharing is considered a promising candidate [2, 3]. Dedicated spectrum allocation in fifth generation (5G) and previous systems results in lower utilization of spectrum resources. With the exponential growth of wireless data traffic, the scarcity of available low-frequency resources becomes more serious [4]. In the case of spectrum sharing between terrestrial 5G cellular networks and fixed satellite service systems, due to the increased probability of non-line-of-sight links for terrestrial terminals and the intermittent nature of uplink transmissions, tens of thousands of terrestrial terminals can be supported simultaneously while meeting the FSS interference protection criteria [5].

In actual deployment scenarios, satellite communication links have the characteristics of long distances. When satellite terminals are located inside buildings or in dense forests, they are susceptible to masking effects that cause line-of-sight (LOS) communications between satellites and terrestrial users to be disrupted. To address the issue of LOS communication disruptions, hybrid satellite-terrestrial relay systems that assist satellite transmissions by deploying terrestrial relays have

attracted considerable research interest in both academia and industry [6]. Recently, terrestrial relay options for relaying signals have attracted considerable interest in hybrid satellite-terrestrial networks, which can increase the channel capacity of satellite links. Several works in the literature have investigated the performance of hybrid satellite terrestrial relay systems using decode-and-forward (DF) [7] and amplify-and-forward (AF) [8] protocols. The hybrid satellite terrestrial system integrating cognitive technology can continuously forward the received signals to mobile users through two cognitive relays for spectrum sharing [9]. Hybrid satellite terrestrial networks can also achieve efficient secondary relay selection through Vickery auctions, and cooperative spectrum sharing schemes are studied under multiple potential secondary relay selection scenarios through an auction-based game method [10]. In a two-hop satellite relay network, channel capacity can be improved by applying multiple antennas to source/destination nodes and using maximum ratio transmission (MRT) and maximum ratio combining (MRC) techniques at the source and destination nodes, respectively [11].

Most existing studies of hybrid satellite-terrestrial systems model the satellite link as Shadow-Rician fading, while assuming that the terrestrial link employs Rayleigh fading or Nakagami-m fading [12]. Furthermore, previous literature always assumes that the hardware of the terminal is perfect. However, the RF front end of hardware circuits often suffers from phase noise, I/Q imbalance, and amplifier nonlinearity [13]. Therefore, hardware impairments (HIs) have an impact on the performance of networks using the AF and DF relay protocols [14]. Reference [15] considers the case of HIs and cochannel interference (CCI), and the outage performance of a hybrid satellite terrestrial network with relay-assisted transmission is also studied. When the terrestrial link adopts Rayleigh fading, closed form analytical and asymptotic expressions for the outage probability (OP) and average channel capacity of the partial relay selection scheme (PRSS) and the opportunistic relay selection scheme (ORSS) are derived. Among them, ORSS selects the relay with the largest instantaneous end-to-end gain of the two-hop link, but synchronization is the key problem in this case, which is difficult to solve for two-hop transmission. However, PRSS selects the maximum gain of one hop, which can greatly reduce the synchronization burden and the complexity of channel state information (CSI) acquisition. Reference [16] analyzed the satellite link with and without direct satellite (DS) link-assisted transmission when the relay forwarding strategy is adopted, deduces the OP expression of the satellite network, and demonstrates the feasibility of spectrum sharing. Reference [17] considers the uplink of a satellite multirelay network, where a single-antenna terminal communicates with the satellite through multiantenna terrestrial relay station using the DF protocol. Due to the spectrum sharing policy, HIs and CCI are considered in the hybrid satellite terrestrial system, and the PRSS scheme is adopted to improve the spatial diversity and enhance the system performance.

Motivated by the above, this paper studies a hybrid satellite terrestrial spectrum sharing system, in which satellite terminals and terrestrial terminals coexist in the same spectrum. Since satellite terminals need to establish communication with satellites and are easily blocked by buildings, this paper mainly considers the research on satellite uplinks. We propose an ORSS scheme for satellite uplinks, which aims to improve the outage performance of satellite networks using DF-based protocol. The DF-based relay selection schemes are decoded at the relay station and has relatively low computational complexity [18]. For evolved 5G and beyond wireless systems, indoor base stations have smaller coverage but greater capacity. Therefore, for satellite terminals subject to masking effect, the base station of the terrestrial network can be rented as the relay station of the satellite link. In addition, in order to alleviate the problem of spectrum scarcity in terrestrial networks, we analyze the cochannel interference effect caused by terrestrial terminals sharing the spectrum of satellite terminals. At the same time, in order to clarify the influence of hardware nonlinear effects on the performance of ORSS mechanism, we introduce the aggregation level of hardware impairments for analysis.

The proposed system may correspond to the scenario of relaying signals when satellite terminals suffer from masking effects in large-scale low earth orbit (LEO) satellite networks. With the aforementioned hybrid satellite terrestrial spectrum sharing system configuration, the satellite link is modeled as Shadowed-Rician fading, and the terrestrial link follows Nakagami-m fading. For the satellite uplink relay and forwarding scheme, the existing literature only considers the performance of the PRSS scheme. Therefore, this paper analyzes the influence of HIs and CCI on the hybrid satellite terrestrial relay network using the ORSS scheme. Furthermore, the PRSS and DS links are used as comparison algorithms to objectively analyze the performance of ORSS scheme. The main contributions of this paper can be summarized as follows:

(i) To address the scarcity of spectrum for terrestrial networks and improve the coverage and stability of satellite communications, we propose a hybrid satellite terrestrial spectrum sharing system based on the ORSS scheme, which relies on the availability of CSI for the relevant links. The optimal relay selection strategy is aimed at minimizing the OP of the system and maximizing the channel capacity on the basis of satellite terrestrial spectrum sharing

(ii) We derive closed-form analytic OP expressions for the satellite uplink when the satellite terminal with and without DS-assisted transmission schemes. Due to spectrum sharing policy and imperfections in the RF front end, we also consider the effects of CCI and HIs. In addition, Monte Carlo (MC) simulations are used to verify the correctness of the OP expression, emphasizing the feasibility of spectrum sharing

(iii) Asymptotic OP expressions for high signal-to-noise ratio (SNR) conditions are also obtained to evaluate the achievable diversity order. We also highlight the

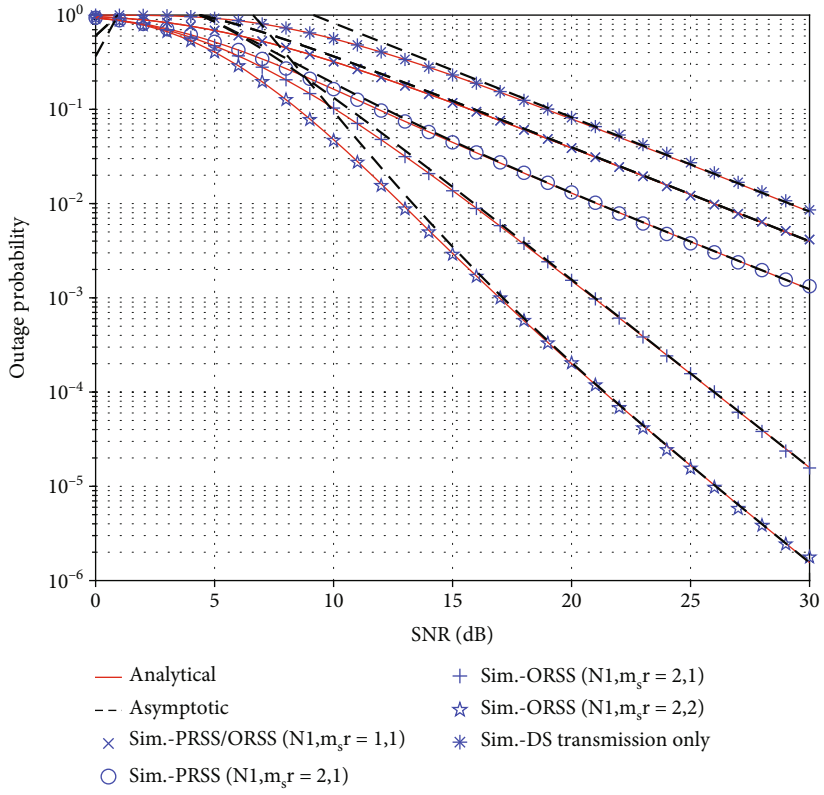

Figure 1: System model.

superiority of the ORSS scheme over the PRSS scheme in terms of OP and throughput performance

The rest of this paper is organized as follows. Section 2 presents a model of a hybrid satellite terrestrial spectrum sharing system with multiple relay stations, describes the hybrid channel model, and formulates the problem. We present the performance analysis of the satellite uplinks with and without DS link-assisted transmission in Section 3. Numerical and simulation results are presented in Section 4. Finally, the conclusions are drawn in Section 5.

2. System Model and Problem Statement

2.1. System Model. The multirelay forwarding scenario of the hybrid satellite-terrestrial network is shown in Figure 1. The scenario includes satellite terminal (S), satellite (D), relay station (R), and terrestrial terminal (C). Assuming that D is a LEO satellite, S and C are fixed service terminals equipped with broadband omnidirectional antennas for receiving and transmitting signals. The Doppler effect of LEO satellites cannot be ignored and can be eliminated by techniques such as Orthogonal Time Frequency Space (OTFS) in signal processing. Therefore, the Doppler effect can be ignored for the subject of spectrum sharing. Assuming that there is a severe fading effect between S and D, terrestrial relays are required to improve the channel capacity. Due to the spectrum sharing strategy, there is CCI caused by M single-antenna terminal terminals. In addition, the satellite terminal has N_1 candidate relay stations that can forward signals. Satellite links are subject to Shadowed-Rician fading, while terrestrial link follows Nakagami-m fading. Specifically, the channel coefficients of the links $S \longrightarrow R$, $S \longrightarrow D$, $C \longrightarrow R$, and $R \longrightarrow D$ are represented by h_{SR_i}, h_{SD}, $h_{C_jR_i}$, and h_{R_iD}, respectively. Furthermore, the receiving nodes in the network are all subject to additive white Gaussian noise (AWGN), where the mean is zero and the variance is σ^2.

2.2. Signal Model. Since the relay station adopts a DF-based protocol and selects the best relay station according to the channel state, the entire communication occurs in two temporal stages. First, satellite terminal S transmits the signal $s(t)$ to the relay R_i and satellite D, where $s(t)$ satisfying $E[|s(t)|^2] = 1$. Therefore, the signal received by the relay station can be expressed as

$$y_{R_i}(t) = \sqrt{P_S} h_{SR_i} w_1^H s(t) + \sum_{j=1}^{M} \sqrt{P_j} h_{C_jR_i} x_j(t) + D_{R_i}(t) + n_{R_i}(t), \tag{1}$$

where P_S is the transmit power at terminal S, P_j denotes the transmit power at interference terrestrial terminal C_j, and $x_j(t)$ is the interference signal with unit average power $E[|x_j(t)|^2] = 1$. $D_{R_i}(t)$ is the distortion noise caused by HIs,

denoted as $D_{R_i}(t) \sim CN(0, K_{SR_i}^2 P_s h_{SR_i}{}^2 + \sum_{j=1}^{M} K_{C_j R_i}^2 P_j h_{C_j R_i}{}^2)$,where K_{SR_i} and $K_{C_j R_i}$ are the aggregate level of HIs of link $S \longrightarrow R_i$ and $C_j \longrightarrow R_i$, respectively. $n_{R_i}(t) \sim \mathcal{CN}(0, \delta_{R_i}^2)$ is the AWGN at relay R_i.

According to equation (1), the received signal-to-noise-plus-interference-distortion ratio (SINDR) of the relay R_i is expressed as

$$\gamma_{SR_i} = \frac{\Lambda_{SR_i}}{K_{SR_i}^2 \Lambda_{SR_i} + \sum_{j=1}^{M} \left(1 + K_{C_j R_i}^2\right) \Lambda_{C_j R_i} + 1}, \tag{2}$$

where $\Lambda_{SR} = \eta_S |h_{SR}|^2$ with $\eta_S = P_S/\sigma^2$ and $\Lambda_{C_j R_i} = \eta_{C_j} |h_{C_j R}|^2$ with $\eta_{C_j} = P_{C_j}/\sigma^2$.

Second, R_i decodes and forwards the received signal $y_{R_i}(t)$ to satellite D. In addition, the DS links have similar transmissions. Thus, the received signal at D can be expressed as

$$y_D(t) = \sqrt{P_J} h_J [s(t) + D_D(t)] + n_D(t), \tag{3}$$

where $J \in (S, R_i)$ and P_J denotes the transmit power at J. $D_D(t)$ is the distortion noise caused by HIs, denoted as $D_D(t) \sim CN(0, K_{JD}^2)$, where K_{JD}^2 is the aggregate level of HIs of link $J \longrightarrow D$. $n_D(t) \sim CN(0, \delta_D^2)$ is the AWGN at satellite D. Therefore, the SINDR at the satellite receiver can be expressed as

$$\gamma_{JD} = \frac{\Lambda_{JD}}{K_{JD}^2 \Lambda_{JD} + 1}, \tag{4}$$

where $\Lambda_{JD} = \eta_J |h_{JD}|^2$ with $\eta_J = P_J/\sigma^2$.

2.3. Channel Model. In practice, it is difficult to obtain an ideal channel state for a satellite link with fast channel variation and large propagation delay. However, the problem of channel estimation and imperfect CSI in hybrid satellite terrestrial systems has been studied in [19–21]. The focus of this paper is to study the performance gains achievable by systems with richer network capabilities, therefore assuming that the two schemes employed in the hybrid satellite terrestrial system have achieved perfect channel conditions to provide system performance benchmarks.

2.3.1. Terrestrial Channel Model. For the hybrid satellite terrestrial spectrum sharing system considered in this paper, the terrestrial link is modeled as Nakagami-m fading channel, and it is assumed that all channels in the system follow quasistatic fading. The channel gain remains constant within each transport block but varies independently from block to block. We assumed that the channel coefficient h_{PR_i}, for $P \in (S, C)$, has a fading severity m_{PR} and average power Ω_{PR}. We can get the probability density function (PDF) and the cumulative distribution function (CDF) of $|h_{PR}|^2$ as

$$f_{|h_{PR_i}|^2}(x) = \left(\frac{m_{PR_i}}{\Omega_{PRi}}\right)^{m_{PR_i}} \frac{x^{m_{PR_i}-1}}{\Gamma(m_{PR_i})} e^{-\left(m_{PR_i}/\Omega_{PR_i}\right)x}, \tag{5}$$

$$F_{|h_{PR_i}|^2}(x) = \frac{\Upsilon\left(m_{PR_i}, m_{PR_i} x/\Omega_{PR_i}\right)}{\Gamma(m_{PR_i})}, \tag{6}$$

where $\Upsilon(\cdot)$ represent the lower incomplete gamma function and $\Gamma(\cdot)$ represent the complete gamma function ([22], eqs. (8.310.1) and (8.350.1)).

Now converting variable $|h_{PR}|^2$ to Λ_{PR}, we can get the PDF of Λ_{PR} as

$$f_{\Lambda_{PR_i}}(x) = \left(\frac{m_{PR_i}}{\Omega_{PR_i}\eta_P}\right)^{m_{PR_i}} \frac{x^{m_{PR_i}-1}}{\Gamma(m_{PR_i})} \cdot e^{-m_{PRi} x/\Omega_{PR_i}\eta_P}. \tag{7}$$

With the help of eq. (3.351.1) in [22], the CDF of Λ_{PR} can be obtained as

$$\begin{aligned} F_{\Lambda_{PR_i}}(x) &= \frac{1}{\Gamma(m_{PR_i})} \Upsilon\left(m_{PR_i}, \frac{m_{PR_i} x}{\Omega_{PR_i}\eta_P}\right) \\ &= 1 - e^{-m_{PR_i} x/\Omega_{PR_i}\eta_P} \sum_{k=0}^{m_{PR_i}-1} \left(\frac{m_{PR_i}}{\Omega_{PR_i}\eta_P}\right)^k \cdot \frac{x^k}{k!}. \end{aligned} \tag{8}$$

2.3.2. Satellite Channel Model. When the satellite link adopts Shadowed-Rician fading model, the PDF of $|h_{QD}|^2$, for $Q \in (S, R_i)$ is given by [23]

$$f_{|h_{QD}|^2}(x) = \alpha_i e^{-\beta_i x} {}_1F_1(m_i; 1; \delta_i x), \quad x \geq 0, \tag{9}$$

where $\alpha_i = (2b_i m_i/(2b_i m_i + \Omega_i))^{m_i}/2b_i$, $\beta_i = 1/2b_i$, and $S_i = \Omega_i/[2b_i(2b_i m_i + \Omega_i)]$, with Ω_i is the average power of LOS component and $2b_i$ is the average power of the multipath component, m_i is the fading severity parameter, and ${}_1F_1(\cdot;\cdot;\cdot)$ is the confluent hypergeometric function of first kind ([22], eq. (9.210.1)). When the fading severity parameter m_i takes an arbitrary integer value, ${}_1F_1(m_i; 1; \delta_i x)$ can be expressed as

$${}_1F_1(m_i; 1; \delta_i x) = e^{\delta_i x} \sum_{\kappa=0}^{m_i-1} \frac{(-1)^\kappa (1 - m_i)_\kappa (\delta_i x)^\kappa}{(\kappa!)^2}, \tag{10}$$

where $(\ )_\kappa$ is the Pochhammer symbol ([22], p. xliii). Substituting (10) into (9) yields a simplified PDF as

$$f_{|h_{QD}|^2}(x) = \alpha_i \sum_{k=0}^{m_i-1} \zeta(k) x^k e^{-(\beta_i-\delta i)x}, \tag{11}$$

with $\zeta(k) = (-1)^k (1-m_i)_k \delta_i^k / (k!)^2$. Now converting variable $|h_{QD}|^2$ to Λ_{QD}, we can get the PDF of Λ_{QD} as

$$f_{\Lambda_{QD}}(x) = \alpha_i \sum_{k=0}^{m_i-1} \frac{\zeta(k)}{\left(\eta_{R_i}\right)^{k+1}} \cdot x^k \cdot e^{-\left((\beta_i-\delta_i)/\eta_{R_i}\right)x}. \tag{12}$$

With the help of eq. (3.351.1) in [22], the CDF of Λ_{R_iD} can be obtained as

$$F_{\Lambda_{QD}}(x) = 1 - \alpha_i \sum_{k=0}^{m_i-1} \frac{\zeta(k)}{(\eta_{Ri})^{k+1}} \sum_{p=0}^{k} \frac{k!}{p!} \left(\frac{\beta_i-\delta_i}{\eta_{R_i}}\right)^{-(k+1-p)} x^p e^{-\left((\beta_i-\delta i)/\eta_{R_i}\right)x}. \tag{13}$$

3. Performance of System

In this section, the analytic outage performance analysis of the hybrid satellite terrestrial spectrum sharing system with and without DS link-assisted transmission is derived. The OP is defined as the probability that the SINDR at the receiver is below a predetermined threshold x_0. In addition, we further deduce the system throughput and asymptotic OP under the condition of high SNR, which can further understand the joint effect of the number of candidate relay stations and fading severity parameter on the diversity order.

3.1. Outage Analysis of Terrestrial Link. According to the complexity of obtaining CSI, the selection schemes of PRSS and ORSS are studied. In addition, from equations (2) and (4), we can get that when $x_0 \geq \min\left(1/K_{SR_i}, 1/K_{R_iD}\right)$ is satisfied, OP is always 1. Therefore, follow-up OP research should be based on the condition $x_0 < \min\left(1/K_{SR_i}, 1/K_{R_iD}\right)$. For a target rate R_p, the OP of the terrestrial link $S \longrightarrow R_i$ under the Nakagami-m fading is given by

$$\begin{aligned} F_{\gamma_{SR_i}}(x_0) &= P\left[\frac{1}{2}\log_2\left(1+\gamma_{SR_i}\right) \leq R_p\right] \\ &= P\left[\frac{\Lambda_{SR_i}}{K_{SR_i}^2 \Lambda_{SR_i} + \sum_{j=1}^{M}\left(1+K_{C_jR_i}^2\right)\Lambda_{C_jR_i}+1} \leq x_0\right] \\ &= \int_0^\infty F_{\Lambda_{SR_i}}\left[\frac{\left(1+K_{CR_i}^2\right)\Lambda_{CR_i}x_0 + x_0}{1-K_{SR_i}^2 x_0}\right] \\ &\quad \times f_{\Lambda_{C_jR_i}}\left(\Lambda_{C_jR_i}\right) d\Lambda_{C_jR}, \end{aligned} \tag{14}$$

where $x_0 = 2^{R_p} - 1$. Assuming that all the aggregate level of HIs $K_{C_jR_i}$ are equal to K_{CR_i}, then $\Lambda_{CR_i} = \sum_{j=1}^{M} \Lambda_{C_jR_i}$ can be obtained.

Lemma 1. *The OP $F_{\gamma_{SR_i}}(x_0)$ can be expressed using equations (7) and (8) as*

$$\begin{aligned} F_{\gamma_{SR_i}}(x_0) = 1 &- \frac{1}{\Gamma\left(m_{C_jR_i}\right)} \left(\frac{m_{C_jR_i}}{\Omega_{C_jR_i}\eta_{C_j}}\right)^{m_{C_jR_i}} e^{-\left[m_{SR_i}x_0/\Omega_{SR_i}\eta_S\left(1-K_{SR_i}^2x_0\right)\right]} \\ &\cdot \sum_{k=0}^{m_{SR_i}-1} \left(\frac{m_{SR_i}}{\Omega_{SR_i}\eta_S}\right)^k \frac{1}{k!} \left(\frac{x_0}{1-K_{SR_i}^2x_0}\right)^k \\ &\cdot \times \sum_{k_2=0}^{k} \binom{k}{k_2} M^{k_2} \left(1+K_{CR_i}^2\right)^{k_2} \Gamma\left(m_{C_jR_i}+k_2\right) \\ &\cdot \left[\frac{m_{C_jR_i}}{\Omega_{C_jR_i}\eta_{C_j}} + \frac{M\left(1+K_{CR_i}^2\right)m_{SR_i}x_0}{\Omega_{SR_i}\eta_S\left(1-K_{SR_i}^2x_0\right)}\right]^{-\left(m_{C_jR_i}+k_2\right)}. \end{aligned} \tag{15}$$

Proof. Please see Appendix A. □

3.2. Outage Analysis of Satellite Link. Using the equation (13), the outage performance of the satellite link $S \longrightarrow D$ and $R \longrightarrow D$ under Shadowed-Rician fading is derived as follows:

$$\begin{aligned} F_{\gamma_{QD}}(x_0) &= P\left(\frac{\Lambda_{QD}}{K_{QD}^2\Lambda_{QD}+1} \leq x_0\right) = F_{\Lambda_{QD}}\left(\frac{x_0}{1-K_{QD}^2x_0}\right) \\ &= 1 - \alpha_i \sum_{k=0}^{m_i-1} \frac{\zeta(k)}{(\eta_{Ri})^{k+1}} \sum_{k_2=0}^{k} \frac{k!}{k_2!} \left(\frac{\beta_i-\delta_i}{\eta_{R_i}}\right)^{-(k+1-k_2)} \\ &\quad \cdot \left(\frac{x_0}{1-K_{QD}^2x_0}\right)^{k_2} e^{-\left(\left((\beta_i-\delta i)/\eta_{R_i}\right)\left(x_0/\left(1-K_{QD}^2x_0\right)\right)\right)}, \end{aligned} \tag{16}$$

where $x_0 = 2^{R_p} - 1$.

3.3. Performance of System without DS Link Utilization. In order to maximize the quality of service of the satellite uplink, the criteria for selecting the best relay station are now discussed. In this section, we conduct the outage probability analysis of the system in the absence of direct satellite link $S \longrightarrow D$ assisted transmission. Furthermore, we deduce the achievable diversity order of the system for the PRSS and ORSS schemes, respectively.

3.3.1. Partial Relay Selection. In particular, based on the channel state of $S - R_i$ links only, the PRSS scheme can be expressed as

$$\gamma_R = \max_{i=1,\cdots,N1} \gamma_{SR_i}. \tag{17}$$

Then, the CDF of γ_R is given by

$$F_{\gamma_R}(x_0) = F_{\gamma_{SR_1}}(x_0) \times \cdots F_{\gamma_{SR_i}}(x_0) \times \ldots F_{\gamma_{SN_1}}(x_0). \tag{18}$$

To balance complexity and performance, each link is assumed to experience the same fading with the PRSS scheme. Therefore, equation (18) can be reexpressed as

$$F_{\gamma_R}(x_0) = \left[F_{\gamma_{SR_i}}(x_0)\right]^{N_1}. \tag{19}$$

Then, the end-to-end SINDR of the uplink hybrid satellite terrestrial system with DF-based protocol is given by

$$\gamma_e = \min\left(\gamma_R, \gamma_{R_iD}\right). \tag{20}$$

Thus, the OP of the system can be given by

$$\begin{aligned} F_{\gamma_e}(x_0) = \Pr(\gamma_e \le x_0) = P(\gamma_R \le x_0) + P\left(\gamma_{R_iD} \le x_0\right) \\ - P(\gamma_R \le x_0)P\left(\gamma_{R_iD} \le x_0\right). \end{aligned} \tag{21}$$

First, insert (15) into (19). Then, substituting $F_{\gamma_R}(x_0)$ and $F_{\gamma_{R_iD}}(x_0)$ into equation (21), the analytic OP $F_{\gamma_e}(x_0)$ of the PRSS scheme can be computed at $x_0 = 2^{R_p} - 1$. While analytic OP expressions can provide many insights in numerical plots, the expressions are too complex to predict the diversity order. Therefore, it is crucial to analyze asymptotic expressions in regions of high SNR, since we can determine the diversity order of the system from the equivalent OP expression. For this, we consider $\eta_S, \eta_{R_i} \longrightarrow \infty$; then, the asymptotic OP for PRSS scheme can be derived.

Lemma 2. *When $\eta_S \longrightarrow \infty$, the asymptotic OP $F^{\infty}_{\gamma_{SR_i}}(x_0)$ can be expressed as*

$$\begin{aligned} F^{\infty}_{\gamma_{SR_i}}(x_0) = \frac{1}{\Gamma\left(m_{SR_i}+1\right)\Gamma\left(m_{C_jR_i}\right)}\left(\frac{m_{SR_i}}{\Omega_{SR_i}\eta_S}\right)^{m_{SR_i}}\left(\frac{x_0}{1-K^2_{SR_i}x_0}\right)^{m_{SR_i}} \\ \times \sum_{k_2}^{m_{SR_i}}\binom{m_{SR_i}}{k_2}\Gamma\left(m_{C_jR_i}+k_2\right)\left(\frac{m_{C_jR_i}}{\Omega_{C_jR_i}\eta_{C_j}}\right)^{-k_2}\left[M\left(1+K^2_{CR_i}\right)\right]^{k_2}. \end{aligned} \tag{22}$$

When $\eta_{R_i} \longrightarrow \infty$, the asymptotic OP $F^{\infty}_{\Lambda_{QD}}(x)$ can be expressed as

$$F^{\infty}_{\gamma_{QD}}(x_0) \simeq \frac{\alpha_i}{\eta_{R_i}}\frac{x_0}{1-K^2_{QD}x_0}. \tag{23}$$

Proof. Please see Appendix B. Through inserting (22) into (19), then substituting $F^{\infty}_{\gamma_R}(x_0)$ and $F^{\infty}_{\gamma_{R_iD}}(x_0)$ into equation (21), the asymptotic OP $F^{\infty}_{\gamma_e}(x_0)$ of the PRSS scheme can be obtained. Finally, with the help of $F^{\infty}_{\gamma_e}(x_0)$, it clearly reflects that the achievable diversity order of the hybrid satellite terrestrial spectrum sharing system is $\min(N_1 m_{SR_i}, 1)$ using PRSS scheme. □

3.3.2. Opportunistic Relay Selection. However, when the CSI of the all $S \longrightarrow R_i$ and $R_i \longrightarrow D$ links is available, the ORSS scheme is designed to maximize the end-to-end SINDR of the system as

$$\gamma_e = \max_{i=1,\cdots,N1} \min\left(\gamma_{SR_i}, \gamma_{R_iD}\right). \tag{24}$$

Thus, we can obtain the OP of the system using the ORSS scheme as

$$\begin{aligned} F_{\gamma_e}(x_0) = \Big[P\left(\gamma_{SR_i} \le x_0\right) + P\left(\gamma_{R_iD} \le x_0\right) \\ - P\left(\gamma_{SR_i} \le x_0\right)P\left(\gamma_{R_iD} \le x_0\right)\Big]^{N_1}. \end{aligned} \tag{25}$$

Then, in order to evaluate the analytic OP for ORSS scheme, $F_{\gamma_e}(x_0)$ can be derived by substituting (15) and (16) into (25).

Similarly, using (22) and (23) in (25), the asymptotic OP $F^{\infty}_{\gamma_e}(x_0)$ for the ORSS scheme can be determined. Based on $F^{\infty}_{\gamma_e}(x_0)$, we infer that the ORSS scheme can achieve the diversity order of N_1.

3.4. Performance of System with DS Link Utilization. In this section, we conduct the OP analysis of the system with the direct $S \longrightarrow D$ link-assisted transmission. Utilizing both the DS link signal and relay signal for MRC, the OP of the satellite terminal's uplink with optimal relay selection is given by

$$P_{\text{out}}\left(R_p\right) = P\left[\log_2(1+\gamma_{SD}+\gamma_e) \le R_p\right] = P(\gamma_{SD}+\gamma_e \le x_0), \tag{26}$$

where $x_0 = 2^{R_p} - 1$ and γ_e is the SINDR of relay transmitted two-hop link. Consequently, we can evaluate (26) as

$$P_{\text{out}}\left(R_p\right) = \int_0^{x_0}\int_0^{x_0-v} f_{\gamma_{SD}}(u) f_{\gamma_e}(v)\,du\,dv. \tag{27}$$

Obtaining an analytical closed-form solution to (27) is difficult by analyzing the PDF expressions of γ_{SD} and γ_e. At this point, an I step staircase approximation can be

made to the actual triangular integral region [24]. Therefore, for sufficiently large I, (27) can be expressed as

$$P_{\text{out}}(R_p) \approx \sum_{i=0}^{I-1}\left[F_{\gamma_{SD}}\left(\frac{i+1}{I}x_0\right) - F_{\gamma_{SD}}\left(\frac{i}{I}x_0\right)\right] \times F_{\gamma_e}\left(\frac{I-i}{I}x_0\right). \tag{28}$$

Therefore, inserting the CDF expressions (21) and (25) into (28), we can compute the analytic OP $P_{\text{out}}(R_p)$ for both PRSS and ORSS schemes, respectively.

Similarly, by substituting the equivalent CDFs $F^{\infty}_{\gamma_{R_iD}}(x_0)$ and $F^{\infty}_{\gamma_e}(x_0)$ into (28), we can get the asymptotic OP $P^{\infty}_{\text{out}}(R_p)$ for PRSS and ORSS schemes with DS link utilization. Thus, we can obtain the achievable diversity order of $1 + \min(N_1 m_{SR_i}, 1)$ and $1 + N_1$ for PRSS and ORSS schemes, respectively.

3.5. Throughput Analysis without DS Link Utilization. In wireless communication, throughput is another key metric for evaluating system performance. In this paper, throughput is defined as the product of the system's target transmission rate R_p and the system connectivity probability $P(\gamma_e \geq x_0)$. For fixed target rate R_p, the overall throughput T_r can be formulated as

$$T_r = R_p \cdot P(\gamma_e \geq x_0) = R_p \cdot \left[1 - F_{\gamma_e}(x_0)\right]. \tag{29}$$

Thus, on inserting the CDF expressions from (21) and (25) into (29), we can compute the analytic throughput T_r for both PRSS and ORSS schemes without DS link-assisted transmission, respectively. Furthermore, to analyze the throughput performance of hybrid satellite terrestrial systems under different fading severity, we consider that satellite links experience infrequent light shadowing (ILS), average shadowing (AS), and frequent heavy shadowing (FHS).

4. Numerical and Simulation Results

In this section, we carry out numerical analysis for the considered hybrid satellite terrestrial system and verify our derived theoretical results through Monte Carlo simulations. First, we use analytical expressions to plot the curves by considering different channel parameters and terminal numbers. In addition, to simplify the analysis, we assume that the terrestrial terminals and relay stations experience independent and identically distributed channels and consider them to be relatively densely clustered [11, 25]. We set $R_p = 0.5$ bps/Hz, so that $x_0 = 1$, $K_{CR_i} = K_{SR_i} = K_{QD} = 0.2$, $M = 1$, $N_1 = [1, 2]$, and interference power $\eta_{C_j} = 2$ dB. The Nakagami-m fading parameters for terrestrial link are considered as $\Omega_{SR_i} = \Omega_{C_jR_i} = 1$, $m_{SR_i} = [1, 2]$, and $m_{C_jR_i} = 1$. The Shadowed-Rician fading parameters for satellite link $R_i \longrightarrow D$ are considered as $\Omega_{R_iD} = 0.279$, $b_{R_iD} = 0.251$, and $m_{R_iD} = 5$ under AS fading condition. The parameters for direct satellite link $S \longrightarrow D$ adopt $\Omega_{SD} = 0.0005$, $b_{SD} = 0.063$, and $m_{SD} = 2$ under FHS fading condition. Furthermore, we set $I = 20$ for the computation of OP without utilization of DS link to make the relative approximation error negligible. In addition, for comparison purposes, the OP curve for benchmark DS link is also plotted in Figure 2.

In Figure 2, we obtain analytical and asymptotic OP curves for the PRSS and ORSS schemes without DS link utilization. We can see that the analytical curve is in good agreement with the simulation results, and the asymptotic curve gradually coincides with the analytical curve at the high SNR region. The respective diversity order of $\min(N_1 m_{SR_i}, 1)$ and N_1 can be verified under the PRSS and ORSS schemes without DS link-assisted transmission. For example, when the (N_1, m_{SR_i}) of PRSS are (1, 1) and (2, 1), the slope of the OP curve proves that the diversity order is 1. Due to bottleneck effect of Shadowed-Rician fading channels, we find that the diversity order of the PRSS scheme is limited to 1. However, the diversity order of 2 can be realized when (N_1, m_{SR_i}) being (2, 1) and (2, 2) for ORSS. In addition, $N_1 = 1$ means that there is only one candidate relay station; thus, the PRSS and ORSS curves coincide. Therefore, we can obtain that under the same network configuration and channel conditions, the outage performance of the ORSS scheme is better than that of the PRSS scheme, and the outage probability of the DS link transmission is the highest.

Figure 3 shows the analytical OP curve for a hybrid satellite terrestrial system with and without DS link and plots asymptotic curves to analyze the diversity order. For the case with DS link utilization, a significant improvement in outage performance can be seen due to the diversity orders of $1 + \min(N_1 m_{SR_i}, 1)$ and $1 + N_1$ for the PRSS and ORSS schemes, respectively. For example, the diversity order of 2 can be realized by analyzing the slopes of the OP curves when (N_1, m_{SR_i}) being (2, 1) for PRSS with DS link utilization and (2, 1) for ORSS without DS link utilization, as compared with (2, 1) for ORSS with DS link utilization with diversity order 3. Thereby, PRSS/ORSS with DS link utilization when (N_1, m_{SR_i}) being (1, 1) can achieve similar performance compared to ORSS without DS link utilization when (N_1, m_{SR_i}) being (2, 1).

Figure 4 plots the OP curve of the system versus SNR η with $x_0 = 1$, $N_1 = 3$, $m_{SR_i} = 1$, and $K_{CR_i} = K_{SR_i} = K_{QD} = [0, 0.3, 0.6]$. Through the slope of the curve, the higher the HI value, the worse the outage performance. Moreover, when the HI level adopts $[0, 0.3]$, the impact of HI on the PRSS/ORSS scheme is small. However, the large value of HIs may have greater impact on the OP of the system. Furthermore, the slope of the OP curve for PRSS can achieve a diversity order of 1 compared to ORSS with a diversity order of 3.

Figure 5 plots the OP curve of the system versus different interference power η_{C_j}, and we assume all η_{C_j} equals to η_C with $\eta_C = [2, 6, 10]$ dB for the PRSS and ORSS schemes. We can get the asymptotic OP curves of the PRSS and ORSS schemes that agree with the Monte Carlo simulation results as the SNR increases. In the high SNR region, the outage performance of the system remains almost same for PRSS schemes with different η_C. Moreover, it can be seen that η_C has a greater impact on the OP of the system using the ORSS scheme. More importantly, when $N_1 = 3$, $m_{SR_i} = 1$, the

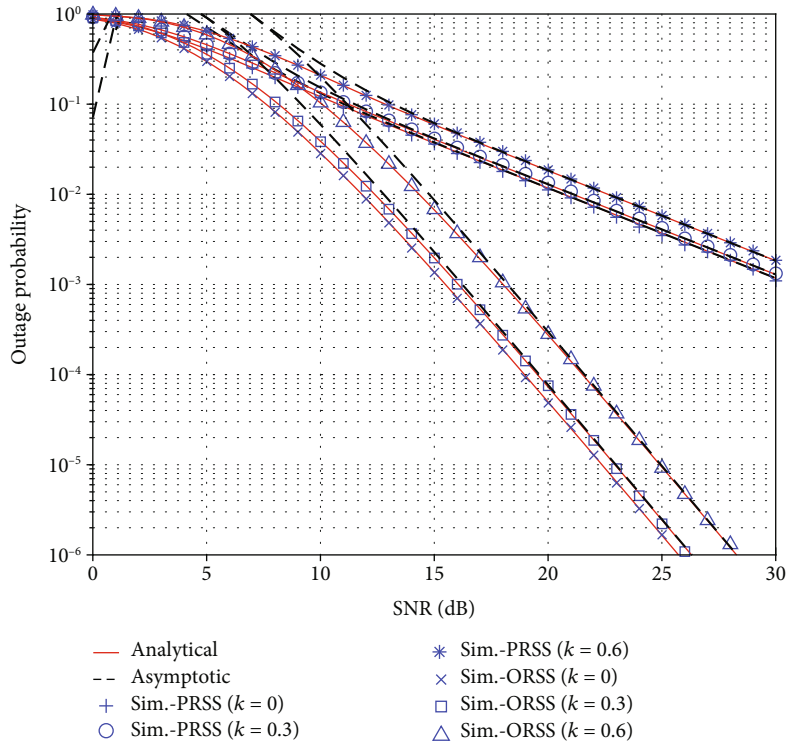

Figure 2: OP of system against SNR.

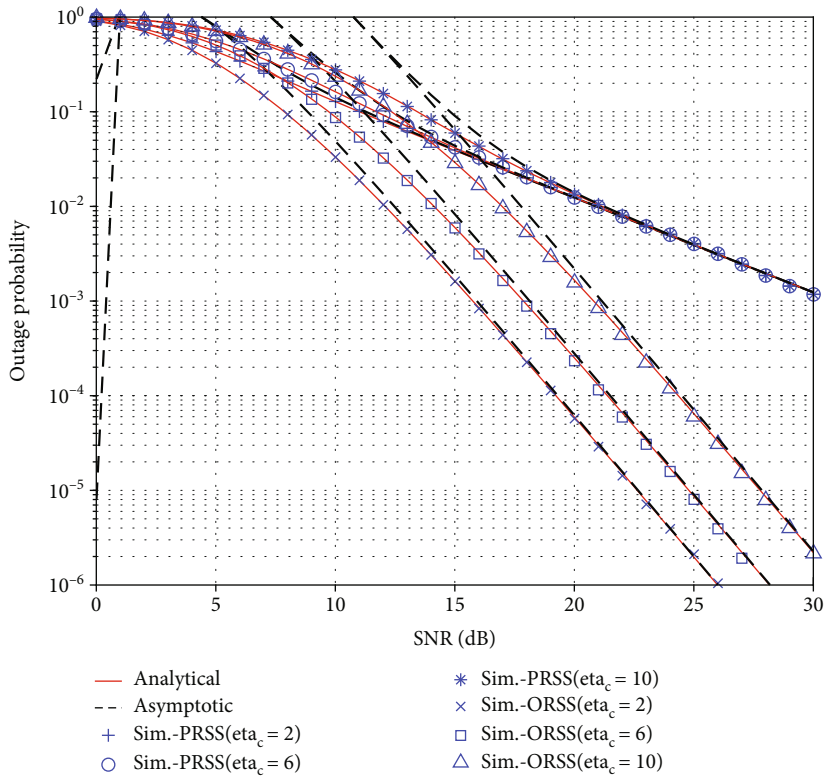

Figure 3: OP of system against SNR with and without DS link assisted.

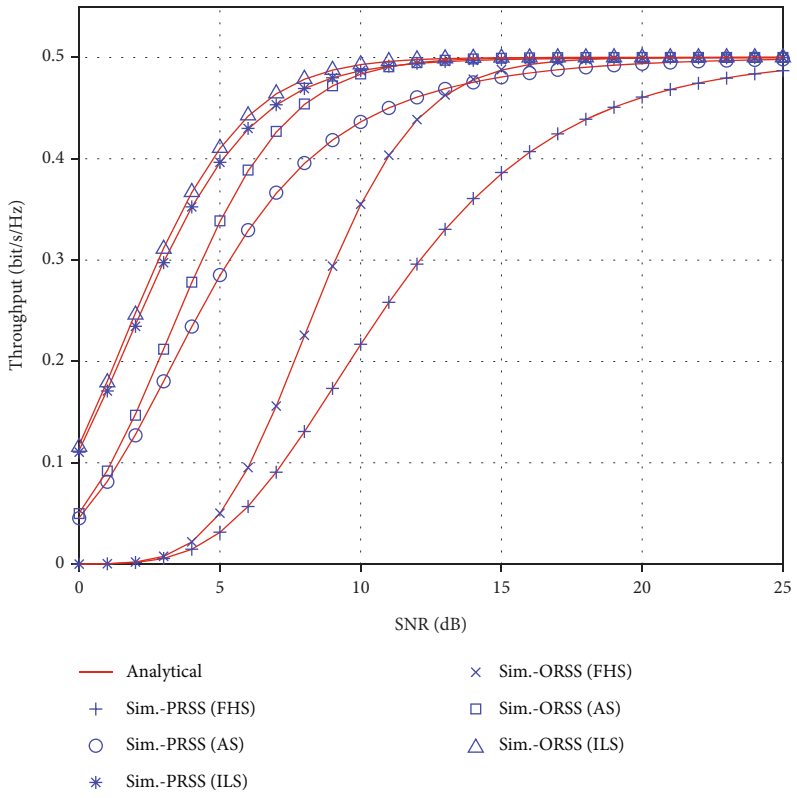

Figure 4: OP of system against SNR with different HIs.

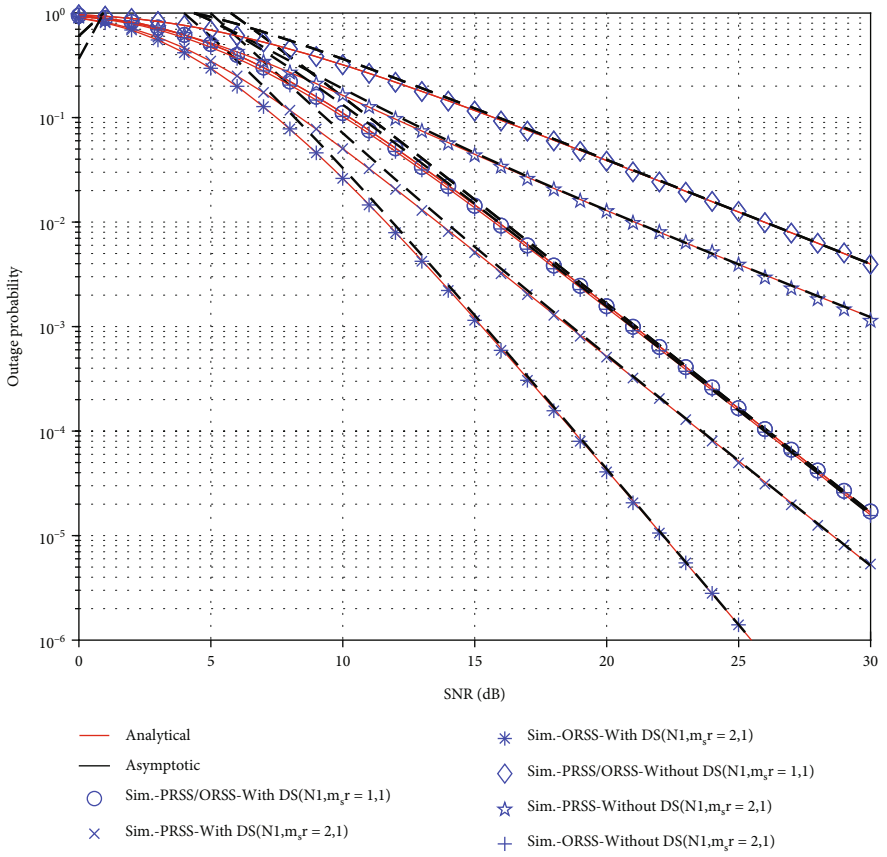

Figure 5: OP of system against SNR with different interference power η_C.

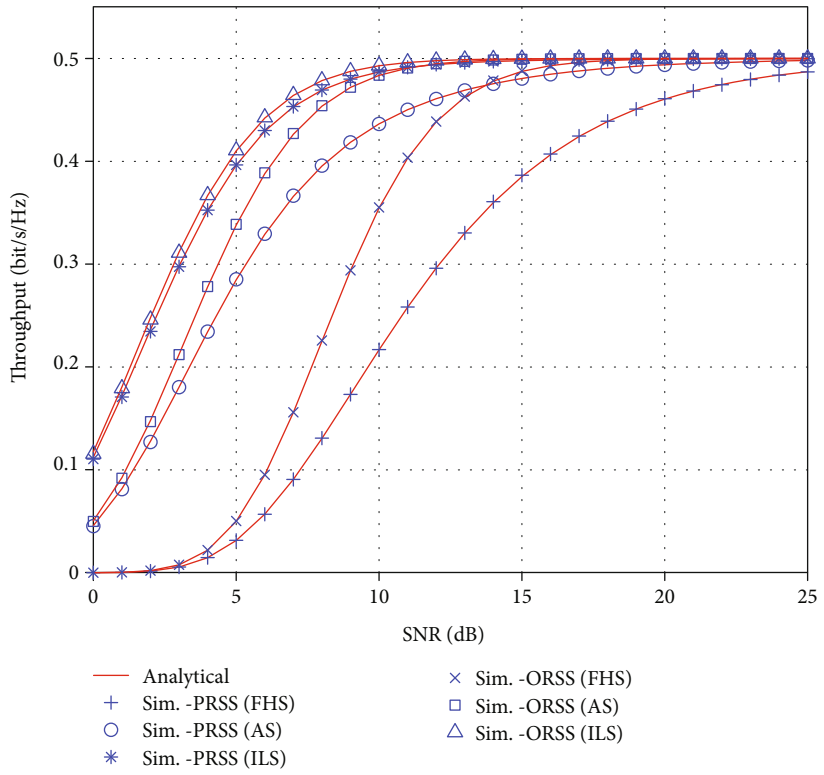

Figure 6: Throughput of system against SNR with different fading severity.

achievable diversity order of min $(N_1 m_{SR_i}, 1)$, N_1 can be verified with these two schemes.

Figure 6 plots the throughput curve of the system under different fading severity, in which we set $R_p = 0.5$ bps/Hz, $N_1 = 3$, and $M = 1$. The parameters for satellite link $R_i \longrightarrow D$ adopt $\Omega_{R_iD} = 1.29$, $b_{R_iD} = 0.158$, and $m_{R_iD} = 10$ under ILS fading condition. It can be seen that the throughput of ORSS converges faster than PRSS under each fading condition, which shows that the ORSS scheme has better robustness against fading. Moreover, the smaller the fading severity of the channel, the greater the throughput of the system, but eventually converges to the target rate of 0.5 bps/Hz.

5. Conclusions

In order to alleviate the scarcity of spectrum resources caused by network expansion, we consider the scenario where terrestrial terminals share the spectrum of satellite terminals. This paper analyzes the outage performance of satellite uplinks with hardware impairments and interference with terrestrial terminals, in which opportunistic relay selection is investigated to improve diversity order. From statistical features on satellite and terrestrial channels, we derive closed-form expressions for the OP and throughput of the system. Furthermore, an asymptotic OP expression is obtained in the high SNR region, and we analyze the achievable diversity order. On this foundation, we have found that the system performance was determined by terrestrial fading severity and the number of candidate relays. However, in contrast to PRSS, the ORSS scheme can achieve higher diversity order under the same channel condition. In addition, the outage performance of the system utilizing the DS link is analyzed by the maximum ratio combination. At the expense of increased receiver complexity, the use of DS link can improve the outage performance of the system. It is worth mentioning that our proposed analysis can provide a useful approach for the design of hybrid satellite terrestrial spectrum sharing system for 5G and beyond networks.

Appendix

A. Proof of link outage probability for satellite terminals

Proof of Lemma 1. On using equations (7) and (8) into (14), $F_{\gamma_{SR_i}}(x_0)$ can be expressed as

$$F_{\gamma_{SR_i}}(x_0) = \int_0^{\infty} \left\{1 - e^{-\left[\left(m_{SR_i}/\Omega_{SR_i}\eta_S\right)\left(\left(1+K_{CR_i}^2\right)\Lambda_{CR_i}x_0 + x_0/\left(1-K_{SR_i}^2x_0\right)\right)\right]} \cdot \sum_{k=0}^{m_{SR_i}-1} \left(\frac{m_{SR_i}}{\Omega_{SR_i}\eta_S}\right)^k \frac{1}{k!} \left[\frac{\left(1+K_{CR_i}^2\right)\Lambda_{CR_i}x_0 + x_0}{1-K_{SR_i}^2x_0}\right]^k\right\} \times \left(\frac{m_{C_jR_i}}{\Omega_{C_jR_i}\eta_{C_j}}\right)^{m_{C_jR_i}} \frac{\Lambda_{C_jR_i}^{m_{C_jR_i}-1}}{\Gamma\left(m_{C_jR_i}\right)} e^{-\left[m_{C_jR_i}\Lambda_{C_jR_i}/\Omega_{C_jR_i}\eta_{C_j}\right]} d\Lambda_{C_jR_i} = I_1 + I_2. \tag{A.1}$$

Referring to the function ([22], 3.351.3), I_1 can be written as

$$I_1 = \frac{1}{\Gamma\left(m_{C_jR_i}\right)}\left(\frac{m_{C_jR_i}}{\Omega_{C_jR_i}\eta_{C_j}}\right)^{m_{C_jR_i}} \cdot \int_0^{\infty} \Lambda_{C_jR_i}^{m_{C_jR_i}-1} e^{-\left[m_{C_jR_i}\Lambda_{C_jR_i}/\Omega_{C_jR_i}\eta_{C_j}\right]} d\Lambda_{C_jR_i} = 1. \tag{A.2}$$

Then, we use the binomial theorem and function ([22], 3.351.3) to solve I_2 as

$$I_2 = \frac{1}{\Gamma\left(m_{C_jR_i}\right)}\left(\frac{m_{C_jR_i}}{\Omega_{C_jR_i}\eta_{C_j}}\right)^{m_{C_jR_i}} \sum_{k=0}^{m_{SR_i}-1}\frac{1}{k!}\left(\frac{m_{SR_i}}{\Omega_{SR_i}\eta_S}\right)^k \underbrace{\times \int_0^{\infty}\left[\frac{\left(1+K_{CR_i}^2\right)\Lambda_{CR_i}x_0 + x_0}{1-K_{SR_i}^2x_0}\right]^k \Lambda_{C_jR_i}^{m_{C_jR_i}-1} e^{-\left[m_{C_jR_i}\Lambda_{C_jR_i}/\Omega_{C_jR_i}\eta_{C_j}\right]} e^{-\left[\left(m_{SR_i}/\Omega_{SR_i}\eta_S\right)\left(\left(1+K_{CR_i}^2\right)\Lambda_{CR_i}x_0 + x_0/\left(1-K_{SR_i}^2x_0\right)\right)\right]} d\Lambda_{C_jR_i}}_{I_3}. \tag{A.3}$$

To simplify the computational analysis, we assume here $\Lambda_{CR_i} = M\Lambda_{C_jR_i}$.

$$I_3 = \sum_{k_2}^{k} M^{k_2}\binom{k}{k_2}\left(\frac{x_0}{1-K_{SR_i}^2x_0}\right)^{k-k_2}\left[\frac{\left(1+K_{CR_i}^2\right)x_0}{1-K_{SR_i}^2x_0}\right]^{k_2} e^{-\left(\left(m_{SR_i}/\Omega_{SR_i}\eta_S\right)\left(x_0/\left(1-K_{SR_i}^2x_0\right)\right)\right)} \underbrace{\cdot \times \int_0^{\infty}\Lambda_{C_jR_i}^{k_2+m_{C_jR_i}-1} e^{-\left[\left(m_{C_jR_i}/\Omega_{C_jR_i}\eta_{C_j}\right)+\left(m_{SR_i}/\Omega_{SR_i}\eta_S\right)\left(M\left(1+K_{CR_i}^2\right)\Lambda_{C_jR_i}x_0/\left(1-K_{SR_i}^2x_0\right)\right)\right]\Lambda_{C_jR_i}} d\Lambda_{C_jR_i}}_{I_4}, \tag{A.4}$$

$$I_4 = \Gamma\left(m_{C_jR_i}+k_2\right)\left[\frac{m_{C_jR_i}}{\Omega_{C_jR_i}\eta_{C_j}} + \frac{m_{SR_i}M\left(1+K_{CR_i}^2\right)x_0}{\Omega_{SR_i}\eta_S\left(1-K_{SR_i}^2x_0\right)}\right]^{-\left(m_{C_jR_i}+k_2\right)} \tag{A.5}$$

Hereby, we can get the desired OP expression of the satellite terminal's terrestrial link. □

B. Proof of asymptotic outage probability for satellite terminals

At high SNR ($\eta_S, \eta_{R_i} \longrightarrow \infty$), we first approximate the terrestrial link under Nakagami-m fading. When $\eta_S \longrightarrow \infty$, we can apply Maclaurin series expansion for the exponential function in (7) to simply the PDF as

$$f_{\Lambda_{RP_i}}(x) = \left(\frac{m_{PR_i}}{\Omega_{PR_i}\eta_P}\right)^{m_{PR_i}} \frac{x^{m_{PR_i}-1}}{\Gamma\left(m_{PR_i}\right)}\sum_{n=0}^{\infty}\left(\frac{1}{n!}\right)\left(-\frac{m_{PRi}x}{\Omega_{PR_i}\eta_P}\right)^n \simeq \left(\frac{m_{PR_i}}{\Omega_{PR_i}\eta_P}\right)^{m_{PR_i}} \frac{x^{m_{PR_i}-1}}{\Gamma\left(m_{PR_i}\right)}. \tag{B.1}$$

Hence, the corresponding CDF of Λ_{PR_i} as

$$F_{\Lambda_{PR_i}}^{\infty}(x) = \frac{1}{\Gamma\left(m_{PR_i}+1\right)}\left(\frac{m_{PR_i}x}{\Omega_{PR_i}\eta_P}\right)^{m_{PR_i}}. \tag{B.2}$$

Then, substituting $F_{\Lambda_{RP_i}}(x)$ and $f_{\Lambda_{RP_i}}(x)$ into equation (14), we can get the asymptotic OP of the terrestrial link as

$$F_{\gamma_{SR_i}}^{\infty}(x_0) = \int_0^{\infty} F_{\Lambda_{SR_i}}\left[\frac{\left(1+K_{CR_i}^2\right)\Lambda_{CR_i}x_0 + x_0}{1-K_{SR_i}^2 x_0}\right] \times f_{\Lambda_{C_jR_i}}\left(\Lambda_{C_jR_i}\right) d\Lambda_{C_jR}$$
$$= \frac{1}{\Gamma\left(m_{SR_i}\right)\Gamma\left(m_{C_jR_i}\right)}\left(\frac{m_{SR_i}}{\Omega_{SR_i}\eta_S}\right)^{m_{SR_i}}\left(\frac{m_{C_jR_i}}{\Omega_{C_jR_i}\eta_{C_j}}\right)^{m_{C_jR_i}} \tag{B.3}$$
$$\times \underbrace{\int_0^{\infty} \Lambda_{C_jR_i}^{m_{C_jR_i}-1}\left[\frac{M\left(1+K_{CR_i}^2\right)\Lambda_{C_jR_i}x_0 + x_0}{1-K_{SR_i}^2 x_0}\right]^{m_{SR_i}} e^{-\left[m_{C_jR_i}\Lambda_{C_jR_i}/\Omega_{C_jR_i}\eta_{C_j}\right]} d\Lambda_{C_jR_i}}_{I_5}.$$

Then, we use the binomial theorem and function ([22], 3.351.3) to solve I_5 as

$$I_5 = \sum_{k_2}^{m_{SR_i}}\binom{m_{SR_i}}{k_2}\left(\frac{x_0}{1-K_{SR_i}^2x_0}\right)^{m_{SR_i}-k_2}\left[\frac{M\left(1+K_{CR_i}^2\right)x_0}{1-K_{SR_i}^2x_0}\right]^{k_2}$$
$$\cdot \int_0^{\infty} \Lambda_{CjR_i}^{m_{C_jR_i}+k_2-1} e^{-\left(m_{C_jR_i}\Lambda_{C_jR_i}/\Omega_{C_jR_i}\eta_{C_j}\right)} d\Lambda_{C_jR_i} =$$
$$= \sum_{k_2}^{m_{SR_i}}\binom{m_{SR_i}}{k_2}\left(\frac{x_0}{1-K_{SR_i}^2x_0}\right)^{m_{SR_i}-k_2}$$
$$\cdot \left[\frac{M\left(1+K_{CR_i}^2\right)x_0}{1-K_{SR_i}^2x_0}\right]^{k_2}\Gamma\left(m_{C_jR_i}+k_2\right)\left(\frac{m_{C_jR_i}}{\Omega_{C_jR_i}\eta_{C_j}}\right)^{-\left(m_{C_jR_i}+k_2\right)}. \tag{B.4}$$

Likewise, for $\eta_{R_i} \longrightarrow \infty$, we can deduce the PDF of satellite link under Shadowed-Rician fading as $f_{\Lambda_{QD}}^{\infty}(x) \simeq (\alpha_i/\eta_{R_i}) + o(x)$ and hence the corresponding CDF as $f_{\Lambda_{QD}}^{\infty}(x) \simeq \alpha_i x/\eta_{R_i}$. Then, inserting $f_{\Lambda_{QD}}^{\infty}(x)$ and $F_{\Lambda_{QD}}^{\infty}(x)$ into $F_{\gamma_{QD}}(x_0)$, we can get

$$f_{\gamma_{QD}}^{\infty}(x_o) = F_{\Lambda_{QD}}\left(\frac{x_0}{1-K_{QD}^2x_0}\right) \simeq \frac{\alpha_i}{\eta_{R_i}}\frac{x_0}{1-K_{QD}^2x_0}. \tag{B.5}$$

Data Availability

The data presented in this study are available on request from the corresponding author.

Conflicts of Interest

The authors declare no conflict of interest.

Acknowledgments

This research was funded by the National Natural Science Foundation of China under grant numbers 62071146 and 62171151 and the Fundamental Research Funds for the Central Universities (No. HIT.OCEF. 2021012).

References

[1] R. Liu, K. Guo, K. An, S. Zhu, C. Li, and L. Gao, "Performance evaluation of NOMA-based cognitive integrated satellite terrestrial relay networks with primary interference," *IEEE Access*, vol. 9, pp. 71422–71434, 2021.

[2] Y. -C. Liang, J. Tan, H. Jia, J. Zhang, and L. Zhao, "Realizing intelligent spectrum management for integrated satellite and terrestrial networks," *Journal of Communications and Information Networks*, vol. 6, no. 1, pp. 32–43, 2021.

[3] Z. Wang, M. Lin, S. Sun, M. Cheng, and W. -P. Zhu, "Robust beamforming for enhancing user fairness in multibeam satellite systems with NOMA," *IEEE Transactions on Vehicular Technology*, vol. 71, no. 1, pp. 1010–1014, 2022.

[4] R. Liu, K. Guo, K. An, S. Zhu, and H. Shuai, "NOMA-based integrated satellite-terrestrial relay networks under spectrum sharing environment," *IEEE Wireless Communications Letters*, vol. 10, no. 6, pp. 1266–1270, 2021.

[5] S. Kim, E. Visotsky, P. Moorut, K. Bechta, A. Ghosh, and C. Dietrich, "Coexistence of 5G with the incumbents in the 28 and 70 GHz bands," *IEEE Journal on Selected Areas in Communications*, vol. 35, no. 6, pp. 1254–1268, 2017.

[6] A. -T. Le, N. -D. X. Ha, D. -T. Do, S. Yadav, and B. M. Lee, "Enabling NOMA in overlay spectrum sharing in hybrid satel-lite-terrestrial systems," *IEEE Access*, vol. 9, pp. 56616–56629, 2021.

[7] X. Zhang, D. Guo, K. An et al., "Performance analysis of NOMA-based cooperative spectrum sharing in hybrid satellite-terrestrial net-works," *IEEE Access*, vol. 7, pp. 172321–172329, 2019.

[8] X. Zhang, B. Zhang, K. An et al., "Outage performance of NOMA-based cognitive hybrid satellite-terrestrial overlay

networks by ampli-fy-and-forward protocols," *IEEE Access*, vol. 7, pp. 85372–85381, 2019.

[9] Z. Li, F. Xiao, S. Wang, T. Pei, and J. Li, "Achievable rate maximization for cognitive hybrid satellite-terrestrial networks with AF-relays," *IEEE Journal on Selected Areas in Communications*, vol. 36, no. 2, pp. 304–313, 2018.

[10] X. Zhang, K. An, B. Zhang, Z. Chen, Y. Yan, and D. Guo, "Vickrey auction-based secondary relay selection in cognitive hybrid satellite-terrestrial overlay networks with non-orthogonal multiple access," *IEEE Wireless Communications Letters*, vol. 9, no. 5, pp. 628–632, 2020.

[11] N. I. Miridakis, D. D. Vergados, and A. Michalas, "Dual-hop communication over a satellite relay and shadowed Rician channels," *IEEE Transactions on Vehicular Technology*, vol. 64, no. 9, pp. 4031–4040, 2015.

[12] H. Kong, M. Lin, J. Zhang, J. Ouyang, W. -P. Zhu, and M. -S. Alouini, "Beamforming design and performance analysis for satellite and UAV integrated networks in IoRT applications," *in IEEE Internet of Things Journal*, vol. 9, no. 16, pp. 14965–14977, 2022.

[13] C. Studer, M. Wenk, and A. Burg, "MIMO transmission with residual transmit-RF impairments," in *2010 International ITG Workshop on Smart Antennas (WSA)*, pp. 189–196, Bremen, Germany, 2010.

[14] V. Singh, S. Solanki, P. K. Upadhyay, D. B. da Costa, and J. M. Moualeu, "Performance analysis of hardware-impaired overlay cognitive satellite–terrestrial networks with adaptive relaying protocol," *IEEE Systems Journal*, vol. 15, no. 1, pp. 192–203, 2021.

[15] T. T. Duy, T. Q. Duong, D. B. da Costa, V. N. Q. Bao, and M. Elkashlan, "Proactive relay selection with joint impact of hard-ware impairment and co-channel interference," *IEEE Transactions on Communications*, vol. 63, no. 5, pp. 1594–1606, 2015.

[16] P. K. Sharma, P. K. Upadhyay, D. B. da Costa, P. S. Bithas, and A. G. Kanatas, "Performance analysis of overlay spectrum sharing in hybrid satellite-terrestrial systems with secondary network selection," *IEEE Transactions on Wireless Communications*, vol. 16, no. 10, pp. 6586–6601, 2017.

[17] K. Guo, K. An, B. Zhang et al., "On the performance of the uplink satellite multiterrestrial relay networks with hardware impairments and interference," *IEEE Systems Journal*, vol. 13, no. 3, pp. 2297–2308, 2019.

[18] H. Kong, M. Lin, J. Zhang, J. Ouyang, J.-B. Wang, and P. K. Upadhyay, "Ergodic sum rate for uplink NOMA transmission in satellite-aerial-ground integrated networks," *Chinese Journal of Aeronautics*, vol. 35, no. 9, pp. 58–70, 2022.

[19] H. Chaouech and R. Bouallegue, "Channel estimation and detection for multibeam satellite communications," in *2010 IEEE Asia Pacific Conference on Circuits and Systems*, pp. 366–369, Kuala Lumpur, Malaysia, 2010.

[20] M. K. Arti, "Channel estimation and detection in hybrid satellite–terrestrial communication systems," *in IEEE Transactions on Vehicular Technology*, vol. 65, no. 7, pp. 5764–5771, 2016.

[21] Z. Zhang, Y. Li, C. Huang et al., "User activity detection and channel estimation for grant-free random access in LEO satellite-enabled Internet of Things," *IEEE Internet of Things Journal*, vol. 7, no. 9, pp. 8811–8825, 2020.

[22] I. S. Gradshteyn and I. M. Ryzhik, *Tables of Integrals, Series and Products*, Academic, New York, NY, USA, 6th ed. edition, 2000.

[23] M. R. Bhatnagar, "Performance analysis of AF based hybrid satellite-terrestrial cooperative network over generalized fading channels," *IEEE Communications Letters*, vol. 17, no. 10, pp. 1912–1915, 2013.

[24] C. Zhang, J. Ge, J. Li, Y. Rui, and M. Guizani, "A unified approach for calculating the outage performance of two-way AF relaying over fading channels," *IEEE Transactions on Vehicular Technology*, vol. 64, no. 3, pp. 1218–1229, 2015.

[25] K. An, M. Lin, and T. Liang, "On the performance of multiuser hybrid satellite-terrestrial relay networks with opportunistic scheduling," *IEEE Communications Letters*, vol. 19, no. 10, pp. 1722–1725, 2015.